MALAYSIAN JOURNAL OF SCIENCE
MJS
ISSN 1394-3065

Regular Issue

Malaysian Journal of Science 43 (3): 119-127 (September 2024) https://mjs.um.edu.my

COMPUTATION OF RAIN-INDUCED ATTENUATION AT CENTIMETRIC WAVE BAND FOR SLANT PATH COMMUNICATION IN NORTH CENTRAL NIGERIA

K.C. Igwe[1a]*, O.D. Oyedum[2a], J.S. Ojo[3b], O.O. Obiyemi[4c], A.G. Ibrahim[5a]

Abstract: This paper examines five globally recognized rain attenuation models for slant path communication to compute the attenuation and identify the models required for optimal rain-induced attenuation prediction over Nigeria's North-Central region. The models considered are Garcia-Lopez, Svjatogor, Bryant, ITU-R P.618-9, and Simple Attenuation. These models have been evaluated for circularly polarized signals in the centimeter wave bands. The Lavergnat-Gole rain rate model was employed to transform the original 5-minute integration time rainfall data to a 1-minute integration time. Attenuation estimates for rain varied widely between 9 and 14 dB for the Ku-band and between 20 and 32 dB for the Ka-band at 0.01% of the time over a typical year. Furthermore, the calculations of the Garcia-Lopez, Bryant, and ITU-R P.618-9 models generally agreed, while the Simple Attenuation and Svjatogor models consistently underestimated the rain-induced attenuation across the selected region and all time percentages.

Keywords: *Slant path, Ka, Ku-band, rain-induced attenuation, north-central Nigeria, rainfall rate*

1. Introduction

Rain attenuation poses the most significant atmospheric threat to the reliability and efficiency of slant path communication systems operating at higher frequency bands (≥ 10 GHz). While degradation from other atmospheric elements such as fog, clouds, snow, and ice occurs, impairments caused by rain are more substantial (Shrestha et al., 2016; Hossain & Islam, 2017; Shrestha & Choi, 2017a; Pérez-García et al., 2023). Consequently, a thorough examination of the impacts of rain degradation on the efficiency of systems operating in high-frequency bands is essential (Shrestha & Choi, 2018).

Attenuation of radio waves propagating through rain occurs due to power absorption in the dielectric medium. Additionally, some losses occur in the directly transmitted wave because of energy scattering by the rain droplets. Scattering losses are typically smaller than those from absorption, depending on the frequency (Collin, 1985).

The inhomogeneity of rain causes complexity in computing rain attenuation. Rain varies greatly in shape, size, and density, leading to no distinct distribution of raindrop sizes for a particular rainfall rate, as it changes temporally and spatially (Tamosiunaite et al., 2010). Accurate analysis of rain attenuation requires precise evaluation of the corresponding rain rate (Oktaviani & Marzuki, 2019). This necessity has been confirmed by recent studies on rain rates (Ng et al., 2017; Shrestha & Choi, 2017b; Rafiqul et al., 2018; Singh & Acharya, 2019).

Due to higher rain intensity and larger raindrops in tropical regions, including Nigeria, signals propagating at centimetric and millimetric wave bands in the tropics are degraded by absorption and scattering during rainfall. Therefore, understanding the extent of rain attenuation in various localities in Nigeria is imperative for satellite system experts to provide quality network services. The Nigerian Communication Satellite (NIGCOMSAT-1R) also utilizes the Ku and Ka bands, and efforts are ongoing to solve the problem of signal outages during rainfall. This is being achieved through various rainfall measurement campaigns and rain attenuation predictions. The present study is part of these efforts.

This paper computes the extent of rain attenuation on slant path communication systems and evaluates the rain attenuation models for optimal predictions in North Central Nigeria. This was achieved using rain data collected at a 5-minute integration time instead of the daily rain data employed in Igwe et al. (2019). It continues the study documented in Igwe (2022) with additional computation of rain attenuation at the Ka-band. Furthermore, results from recent efforts in North Central Nigeria align with the present study (Alozie et al., 2022; Isabona et al., 2022a; Isabona et al., 2022b; Igwe, 2023).

Authors information:
[a]Department of Physics, Federal University of Technology, Minna, Niger State, NIGERIA. E-mail: k.igwe@futminna.edu.ng[1]; onyedidavid@futminna.edu.ng[2]; ibrahimaku@ futminna.edu.ng[5]
[b]Department of Physics, Federal University of Technology, Akure, Ondo State, NIGERIA. E-mail: ojojs_74@futa.edu.ng[3]
[c]Department of Electrical/Electronic Engineering, Osun State University, NIGERIA. E-mail: obiseye.obiyemi@uniosun.edu.ng[4]
*Corresponding Author: k.igwe@futminna.edu.ng

Received: October 11, 2022
Accepted: June 20, 2023
Published: September 30, 2024

DOI:https//doi.org/10.22452/mjs.vol43no3.13
Malaysian Journal of Science 43(3): 119-127 (September 2024)

2. Background

Rain Rate Statistics and Conversion Model

The Lavergnat and Gole (L-G) rain rate conversion model has been widely employed since its development (Lavergnat & Gole, 1998). This model was used to analyze rainfall rates for this investigation because it has recently proven to be the most effective rainfall rate conversion tool for the zone under consideration (Igwe et al., 2021). The conversion of rainfall rate distribution from a given data acquisition time (integration time) t_1 to the required equivalent time of integration t_2 is facilitated by this model. This is accomplished using a conversion factor of the ratio t_2 to t_1 (Lavergnat & Gole, 1998):

$$Pr_2(R_2) = (CF)^a Pr_1(R_1) \quad (1)$$

where $$CF = \frac{t_2\,(\text{min})}{t_1(\text{min})} \quad (2)$$

and $$R_2(mm/h) = \frac{R_1(\text{mm/h})}{(CF)^a} \quad (3)$$

where Pr_1 and Pr_2 are the probabilities realised with rain gauges at t_1 and t_2 respectively, while the rain rates for Pr_1 and Pr_2 are represented by R_1 and R_2.

The region of interest relies on the parameter 'a', which has an estimate of 0.115 for the temperate region, with 0.143 being the equivalent estimate for the tropical climatic region, as quantified by Emiliani *et al*. (2009).

The Selected Models for Rain-Induced Attenuation

Five widely recognized models for estimating rain attenuation were employed in this study. These are the Bryant model, the Garcia-Lopez (G-L) model, the internationally recognized ITU-R P.618-9 model (ITU-R model), the Simple Attenuation Model (SAM), and the Svjatogor model. Detailed explanations can be found in Igwe et al. (2019); however, the models are briefly defined below.

***The ITU-R model*:** This model uses the rainfall rate that exceeded 0.01% to predict rain attenuation. For other percentage exceedances, an adjustment factor is applied. The computational steps are detailed in ITU-R (2007).

***The Bryant Model**:* Derived by Bryant et al. (1999), this model calculates rain attenuation distribution based on the concept of an effective rain cell and variable rain height.

***The Garcia-Lopez Model**:* Developed to predict rain attenuation on slant-path links, this model uses coefficients specific to tropical regions (Garcia-Lopez et al., 1988).

The Simple Attenuation Model: Stutzman and Dishman derived this model in 1984. It is based on an exponentially shaped rain rate profile and incorporates characteristics of both convective and stratiform rain types.

***The Svjatogor Model**:* This model, derived by Svjatogor (1985), is unique in that its effective rain height depends on the measured rain intensity.

The parameters inputted into the attenuation models used are listed in Table 1.

Table 1. Parameters used in the attenuation models

Attenuation model	H_S	θ	λ	f	k, α	$R_{0.01}$	$R_P(p)$
ITU-R	√	√	√	√	√	√	
G-L	√	√	√		√		√
Bryant	√	√			√		√
Svjatogor	√	√			√		√
SAM	√	√	√		√		√

where H_S: Station's altitude (km), θ: elevation angle (°), λ: Station's latitude (°), f: frequency (in GHz), k and α: Coefficients dependent on frequency and polarisation (ITU-R, 2005), $R_{0.01}$ (mm/h): Point rain rate at 0.01%, p: Percentage time of the year (%), $R_p(p)$: Point rain rate (mm/h).

3. Methodology

Part of the rainfall data used in this study was collected at 5-minute integration intervals from the Tropospheric Data Acquisition Network (TRODAN) situated at the Federal University of Technology, Minna, Nigeria. Additional rainfall data were obtained from the Centre for Atmospheric Research (CAR), Anyigba, Nigeria. The CAR stores rainfall data collected from other locations with TRODAN stations, such as Benue State University, Makurdi; University of Abuja; University of Jos; and Kogi State University, Anyigba. The North Central region of Nigeria comprises six states and the Federal Capital Territory (FCT), Abuja. However, rainfall data were obtained from only four states, including Abuja, as TRODAN weather stations have not been installed in the remaining two states, Kwara and Nasarawa. The rainfall data obtained from the five locations ranged between 2 and 4 years.

The data were collected using a tipping bucket rain gauge and a Campbell CR-1000 data logger. The rain gauge measures rainfall at 5-minute integration intervals, necessitating the conversion of the measured data to 1-minute integration intervals. The data logger can measure almost any sensor with an electrical response, recording the signals and converting the measurements to engineering units. The CR-1000 data logger and tipping bucket rain gauge in the TRODAN station are shown in Figure 1.

DOI:https//doi.org/10.22452/mjs.vol43no3.13
Malaysian Journal of Science 43(3): 119-127 (September 2024)

Figure 1. (a) The outdoor TRODAN measuring console equipped with a CR-1000 data acquisition system (b) The TRODAN in-situ measuring rain gauge

The 5-minute rain rate (mm/h) statistics were converted to a 1-minute rainfall rate (mm/h) equivalent using the L-G model discussed in section 2. The attenuation models outlined in section 2 were employed to compute the rain attenuation values. Circular polarisation was used to examine the downlink centre frequencies of 12.68 GHz and 19.45 GHz for the Ku- and Ka-bands, respectively. This followed the interpolation of the horizontal and vertical polarisation values of k and α at both frequencies (Ajewole, 1997). Elevation angles of 55 degrees and 42.5 degrees were used. Satellite receivers in Nigeria employ these two angles: 55 degrees for the Atlantic Ocean Region (AOR) and 42.5 degrees for NIGCOMSAT-1R reception across the AOR. Figure 2 provides the flow diagram of the methodology.

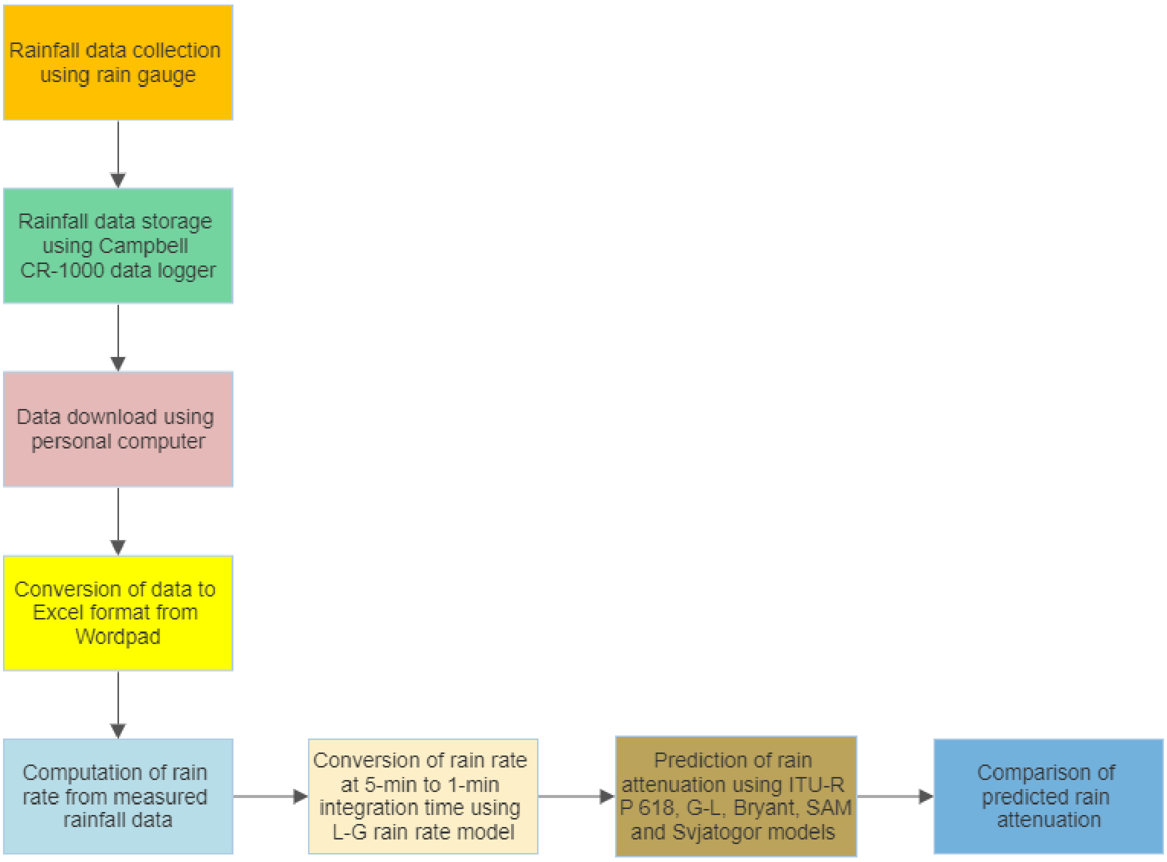

Figure 2. Flow diagram of methodology

DOI:https//doi.org/10.22452/mjs.vol43no3.13
Malaysian Journal of Science 43(3): 119-127 (September 2024)

4. Results and Discussion

Rainfall Rate Computation

Table 2 presents the preliminary requirements for rain attenuation that must be satisfied.

Table 2. Station parameters and converted rain rate

Location	Lat (°N)	Long (°E)	Alt (m)	$R_{0.01}$ (mm/h)
Abuja	9.00	7.28	334	44.00
Anyigba	7.25	7.18	420	37.80
Jos	9.58	8.57	1110	75.50
Makurdi	7.70	8.50	142	75.50
Minna	9.54	6.54	249	75.50

According to Table 2, the maximum $R_{0.01}$ is 75.50 mm/h, which is recorded in three stations, Jos, Makurdi and Minna. Meanwhile, the minimum $R_{0.01}$ is 37.80 recorded in Anyigba.

Rain Attenuation Computation

The computed attenuation using the aforementioned models was compared against the ITU-R model, which serves as the standard due to its global acceptance for accuracy. It is common practice to compare estimated rain attenuation values from various models to the ITU-R model in the absence of direct observations (Abayomi & Khamis, 2012). Research findings confirm that ITU-R model computations align with direct measured values (Mandeep & Allnut, 2007; Ojo et al., 2008; Panchal & Joshi, 2016; Hossain & Islam, 2017).

Rain attenuation computation depends on numerous parameters, some of which are shown in Table 1. Other crucial parameters include rain height (Hr), slant path length (Ls), effective path length (Le), and horizontal projection (Lg). Accurate computation of these parameters ensures precise calculation of the corresponding rain attenuation. Therefore, these relevant input parameters were determined as a prerequisite for rain attenuation prediction. Tables 3 and 4 present the values of these parameters at the two super-high frequency bands (Ku and Ka).

Table 3. Parameters for computation at 55°

Location	H_r (km)	L_s (km)	L_g (km)	L_e_Ku (km)	L_e_Ka (km)
Abuja	4.76	5.40	3.10	4.72	5.18
Anyigba	4.75	5.28	3.03	5.04	5.46
Jos	4.76	4.45	2.55	3.22	3.65
Makurdi	4.76	5.64	3.23	3.68	4.19
Minna	4.79	5.54	3.18	3.61	4.13

Table 4. Parameters for computation at 42.5°

Location	H_r (km)	L_s (km)	L_g (km)	L_e_Ku (km)	L_e_Ka (km)
Abuja	4.76	6.55	4.83	4.89	5.30
Anyigba	4.75	6.41	4.72	5.25	5.62
Jos	4.76	5.40	3.98	3.30	3.70
Makurdi	4.76	6.84	5.04	3.75	4.23
Minna	4.79	6.72	4.95	3.67	4.15

It is observed from Tables 3 and 4 that the computed values of H_r, L_s, L_g and L_e increase as the elevation angles decrease from 55° to 42.5° in all locations, and at both frequency bands considered. It is also noticed that computed values are higher at Ka than at Ku.

Table 5 shows the computed rain attenuation at Ku, 55° elevation angle.

Table 5. Computed rain attenuation at Ku, 55° elevation angle

% time Exceedance	Station	ITU-R P.618-9 (dB)	Bryant (dB)	Garcia-Lopez (dB)	SAM (dB)	Svjatogor (dB)
0.001	Abuja	16.0	13.0	11.0	2.3	8.2
	Anyigba	15.0	12.0	9.0	1.7	7.7
	Jos	19.5	16.0	17.0	4.1	6.9
	Makurdi	21.5	19.5	18.0	2.5	12.7
	Minna	21.5	19.5	18.0	2.7	12.3
0.01	Abuja	10.0	8.0	6.5	1.1	4.6
	Anyigba	9.0	7.0	5.6	0.8	4.4
	Jos	12.0	9.7	10.6	2.1	3.8
	Makurdi	13.8	12.0	11.0	1.2	7.6
	Minna	13.5	12.0	11.0	1.4	7.2
0.1	Abuja	3.3	3.2	2.6	0.4	1.8
	Anyigba	3.0	3.0	2.3	0.3	1.7
	Jos	4.0	4.0	4.5	0.7	1.4
	Makurdi	5.0	5.0	5.0	0.4	3.2
	Minna	6.0	5.0	5.0	0.5	3.0
1	Abuja	0.8	0.6	0.5	0.1	0.3
	Anyigba	0.7	0.5	0.4	0.0	0.3
	Jos	1.0	0.8	0.8	0.1	0.2
	Makurdi	1.2	1.0	0.9	0.1	0.6
	Minna	1.1	1.0	0.9	0.1	0.5

DOI:https//doi.org/10.22452/mjs.vol43no3.13
Malaysian Journal of Science 43(3): 119-127 (September 2024)

Table 5 shows that locations with similar rain rate values at 0.01% (as recorded in Table 2) also exhibit similar attenuation values. This trend is particularly noticeable in Makurdi and Minna, both of which recorded the highest rainfall rate of 75.5 mm/h at 0.01%. Consequently, the maximum attenuation values at 0.01% of the year are 13.8 dB for Makurdi and 13.5 dB for Minna, as computed by the ITU-R model. A relatively close attenuation value was also recorded at the Jos station, which has a similar rain rate. Conversely, a minimum attenuation value of 9 dB is predicted for Anyigba, corresponding to its lower rainfall rate.

It is further observed that the Bryant and G-L model computations closely align with the ITU-R model, especially at higher percentage exceedances of 0.1% and 1%. The deviation here ranges from 0.1 to 1 dB, whereas the differences at lower percentage exceedances of 0.001% and 0.01% are about 2-5 dB. Predictions by the Svjatogor model and SAM deviate significantly from the others.

The predicted attenuation at Ku, 42.5° is presented in Figures 3(a)-(e).

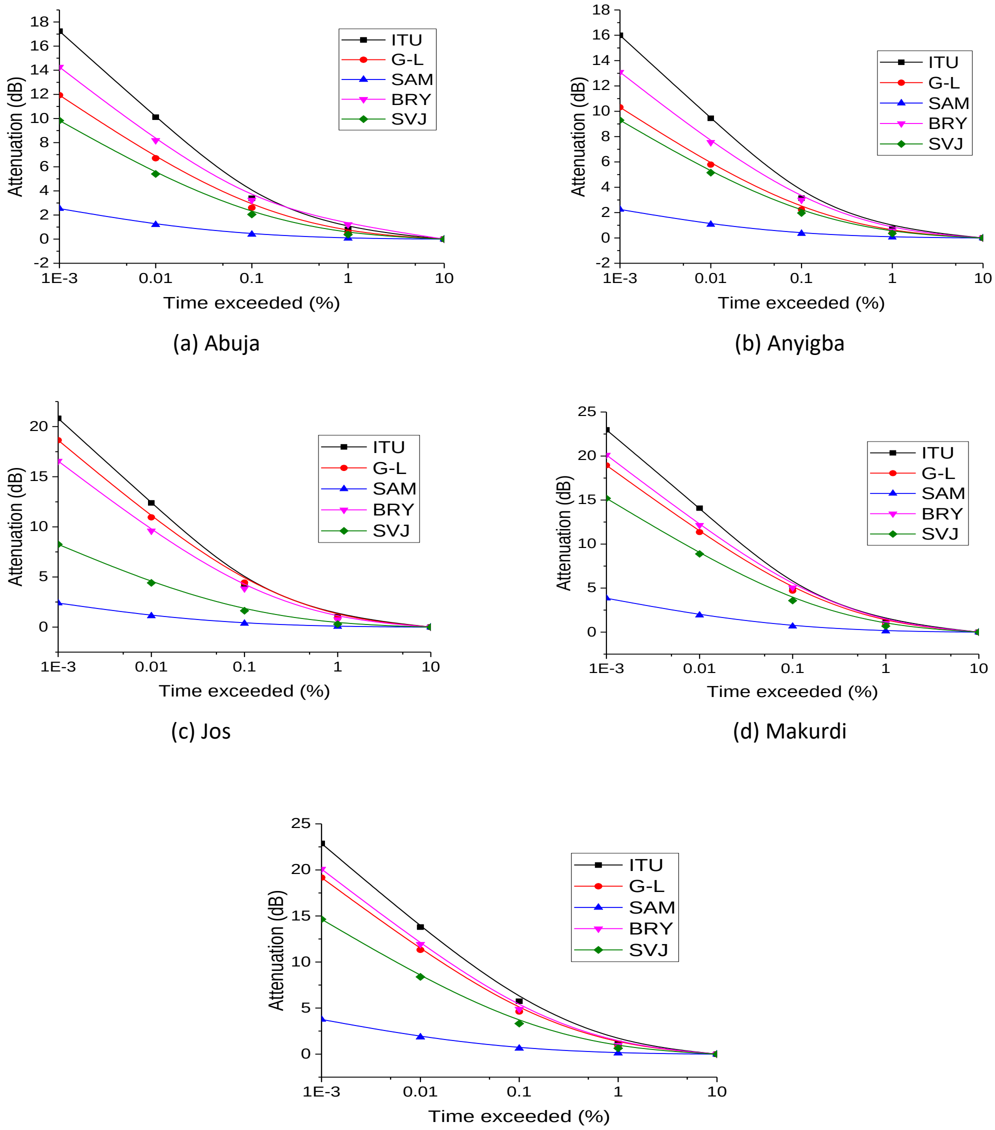

(a) Abuja (b) Anyigba (c) Jos (d) Makurdi (e) Minna

Figure 3. Computed attenuation at Ku, 42.5° look angle

As depicted in Figure 3, the computed attenuation values at 42.5° are slightly higher than those computed at 55°, with a 2-5 dB deviation across the entire distribution. Furthermore, the estimations by the Bryant and G-L models align closely with the ITU-R model, particularly at higher time percentage exceedances. In contrast, the predicted values from the SAM and Svjatogor models consistently underestimate the computed attenuation at every percentage of time.

DOI:https//doi.org/10.22452/mjs.vol43no3.13
Malaysian Journal of Science 43(3): 119-127 (September 2024)

Table 6 shows the computed attenuation at Ka-band, 55° elevation angle.

Table 6. Computed attenuation at Ka, 55° look angle

% time Exceedance	Stations	ITU-R P.618-9 (dB)	Bryant (dB)	Garcia-Lopez (dB)	SAM (dB)	Svjatogor (dB)
0.001	Abuja	33.3	25.3	21.3	3.0	15.6
	Anyigba	30.1	23.0	18.6	2.7	14.8
	Jos	40.5	29.8	32.3	9.5	12.8
	Makurdi	45.0	36.1	32.9	10.5	23.6
	Minna	45.1	36.2	33.3	10.5	22.8
0.01	Abuja	22.1	16.3	13.5	1.5	9.5
	Anyigba	20.4	15.0	11.7	1.4	9.2
	Jos	27.3	19.4	21.2	5.4	7.6
	Makurdi	31. 4	24.6	22.1	6.2	15.3
	Minna	31.0	24.1	22.0	6.1	14.4
0.1	Abuja	8.0	7.2	5.9	0.5	4.0
	Anyigba	7.4	6.6	5.1	0.5	3.9
	Jos	10.1	8.7	9.6	2.1	3.1
	Makurdi	11.8	11.5	10.2	2.5	6.8
	Minna	14.5	11.1	10.0	2.4	6.3
1	Abuja	2.1	1.4	1.1	0.1	0.7
	Anyigba	1.9	1.3	1.0	0.1	0.7
	Jos	2.7	1.8	2.0	0.4	0.6
	Makurdi	3.1	2.3	2.1	0.4	1.3
	Minna	3.1	2.3	2.0	0.4	1.2

Table 6 shows that attenuation computed at the Ka-band is substantially higher than at the Ku-band. The maximum attenuation value exceeded at 0.01% of the year is 31 dB, as computed by the ITU-R model for Makurdi and Minna, while the minimum value of 20.4 dB is predicted for Anyigba. The computed values by the G-L and Bryant models are close to those computed by the ITU-R model, albeit with higher deviations. At higher percentage exceedances of 0.1% and 1%, the deviations in computed attenuation range between 1 and 3 dB, whereas at lower percentage exceedances of 0.001-0.01%, the deviations are in the 5-11 dB range. The SAM and Svjatogor models again underestimate the computed values at every percentage of time. Predictions by these two models deviate significantly from the others, with differences at higher percentage exceedances of 0.1% and 1% ranging from 2 to 12 dB, while computed attenuation at lower percentage exceedances of 0.001-0.01% ranges from 11 to 22 dB.

DOI:https//doi.org/10.22452/mjs.vol43no3.13
Malaysian Journal of Science 43(3): 119-127 (September 2024)

Figures 4(a)-(e) show the computed attenuation at Ka, 42.5° elevation angle.

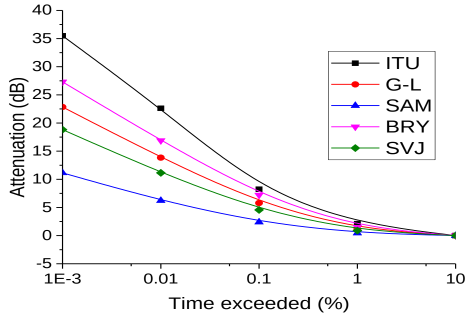

(a) Abuja

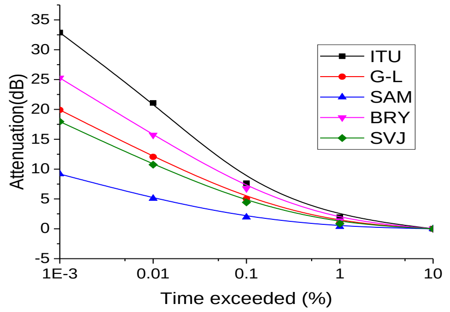

(b) Anyigba

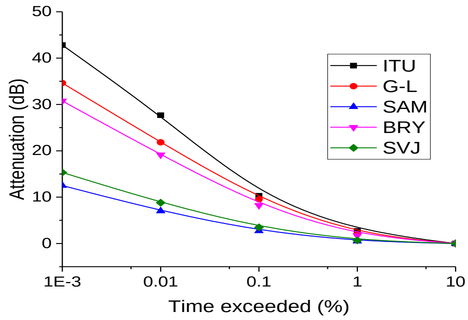

(c) Jos

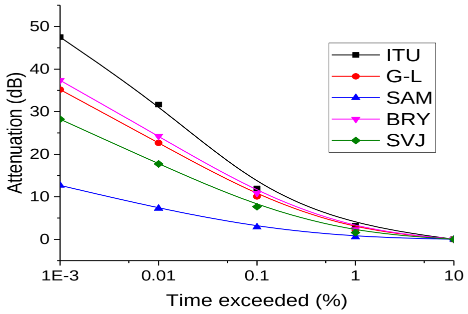

(d) Makurdi

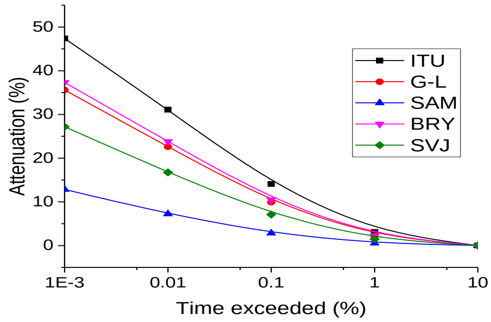

(e) Minna

Figure 4. Computed attenuation at Ka-band, 42.5° elevation angle

As seen in Figure 4, the computed values of rain attenuation at 42.5° are slightly higher compared to those obtained at 55°. At 0.01%, attenuation varies between a minimum value of 21.1 dB, predicted for Anyigba, and a maximum value of 31.7 dB, predicted for Makurdi, as computed by the ITU-R model. At the Ka-band, predictions by the Bryant and G-L models closely match the ITU-R model only at higher percentage exceedances of 0.1% and 1%. All four models underestimate the computed attenuation at lower percentage time exceedances of 0.001% and 0.01%.

5. Conclusion

Computations of rain attenuation on slant path links at super high frequency (SHF) bands (Ku and Ka) were conducted using five commonly employed models for rain attenuation prediction: Bryant, Garcia-Lopez, ITU-R P.618-9, Simple Attenuation, and Svjatogor. These computations were performed at elevation angles of 55° and 42.5°. The findings revealed that higher rainfall rates resulted in greater rain attenuation, and higher attenuation was observed at lower percentage time exceedances. At the examined elevation angles, lower attenuation values were obtained at 55°, while higher values were noted at 42.5°, indicating that higher elevation angles are generally associated with lower attenuation. Additionally, the results indicated that rain attenuation values were significantly higher at the Ka-band than at the Ku-band, suggesting that attenuation increases with frequency. At the Ku-band, attenuation ranged from 9 to 14 dB at both 55° and 42.5° at 0.01% time exceedance. At the Ka-band, attenuation ranged from 20 to 31 dB at 55° and 21 to 32 dB at 42.5° at 0.01% time exceedance.

Furthermore, the Bryant, Garcia-Lopez, and ITU-R P.618-9 models showed good agreement, especially at the Ku frequency band. However, at the Ka frequency band, deviations among these three models were lower at higher percentage exceedances

DOI:https//doi.org/10.22452/mjs.vol43no3.13
Malaysian Journal of Science 43(3): 119-127 (September 2024)

(0.1% and 1%) than at lower exceedances (0.001% and 0.01%) for the entire distribution. The SAM and Svjatogor models consistently underestimated the computed rain attenuation values for every percentage of time. Therefore, the Bryant, Garcia-Lopez, and ITU-R P.618-9 models could be effectively used to compute rain attenuation at the Ku-band and at higher percentage exceedances of the Ka-band in the North Central region of Nigeria.

A limitation of this study is the inability to corroborate the predicted rain attenuation with actual signal attenuation measurements. However, the values computed using the ITU-R P.618 model, which served as the standard, were consistent with the model's validation examples for prediction methods.

6.Acknowledgement

The authors thank the Centre for Atmospheric Research (CAR), Anyigba, Nigeria for making the data used in this work available.

7. References

Abayomi Y.I.O., Khamis N.H.H. (2012). Rain attenuation modelling and mitigation in the tropics: Brief review. *Int. J. of Elect. and Comp. Eng*., 2(6), 748-757.

Ajewole, M. O. (1997). Scattering and attenuation of centimeter and millimetre radio signals by tropical rainfall. *Ph.D thesis, Federal University of Technology, Akure, Nigeria.*

Alozie, E., Abdulkarim, A., Abdullahi, I., Usman, A.D., Faruk, N., Olayinka, I.-F.Y., Adewole, K.S., Oloyede, A.A., Chiroma, H., Sowande, O.A., *et al* (2022). A review on rain signal attenuation modeling, analysis and validation techniques: Advances, challenges and future direction. *Sustainability,* 14, 11744, 1-65.

Bryant G.H., Adimula I., Riva C., Brussard G. (1999). Rain attenuation statistics from rain column, diameters and heights. *Int. J. of Sat. Commun*., 19, 263-283.

Collin R. E. (1985). *Antennas and radiowave propagation*. McGraw-Hill international editions, electrical engineering series, Singapore, 339-409.

Emiliani L. D., Luini L. & Capsoni C. (2009). Analysis and parameterization of methodologies for the conversion of rain-rate cumulative distributions from various integration times to one minute. *IEEE Antennas and Propagation Magazine*, 51(3), 70–80.

Garcia-Lopez J.A., Hernando J.M., Selga J. (1988). Simple rain attenuation method for satellite radio links. Year-to-year variability of rainfall for microwave applications in the USA. *IEEE Trans. on Ant. and Propag*., 36(3), 444-448.

Hossain M.S., Islam M.A. (2017). Estimation of rain attenuation at EHF bands for earth-to-satellite links in Bangladesh. *Int. Conf. on Elect., Comp. and Commun. Eng. (ECCE)*, Cox's Bazar, Bangladesh, 589-593.

Igwe K. C., Oyedum O. D., Ajewole M. O., Aibinu A. M. (2019). Evaluation of some rain attenuation prediction models for satellite communication at Ku and Ka bands. *Journal of Atmospheric and Solar-Terrestrial Physics*, 188, 52–61.

Igwe K.C., Oyedum O.D, Ajewole M.O, Aibinu A.M, Ezenwora J.A. (2021) Performance evaluation of some rain rate conversion models for microwave propagation studies. *Adv Space Res* 67:3098-3105.

Igwe K. C. (2022). Optimal rain attenuation prediction models for earth-space communication at Ku-band in North Central Nigeria. Proceedings of the 7th International Conference on the Applications of Science and Mathematics. *Springer Proceedings in Physics,* 273, 415-428.

Igwe K. C. (2023). Derivation of regression coefficients and conversion factors for 1-minute rain rate statistics in a tropical environment. *Journal of Advanced Industrial Technology and Application,* 4 (1), 29-37.

ITU-R (2005). Specific attenuation model for rain for use in prediction methods. *Rec. P.838-3, ITU-R P Sers., Int. Telecomm, Union*, Geneva.

ITU-R 2007. Propagation data and prediction methods required for the design of earth–space telecommunication systems. *Rec. P.618-9, ITU-R P Sers., Int. Telecomm, Union,* Geneva.

Isabona, J., Imoize, A.L., Rawat, P., Jamal, S.S., Pant, B., Ojo, S., Hinga, S.K. (2022). Realistic prognostic modeling of specific attenuation due to rain at microwave frequency for tropical climate region. *Wireless Communications and Mobile Computing (Wiley-Hindawi)*, 1-10.

Isabona, J., Imoize, A.L., Ojo, S., Lee, C.-C., Li, C.-T. (2022). Atmospheric propagation modelling for terrestrial radio frequency communication links in a tropical wet and dry savanna climate. *Information*, 13 (141), 1-16.

Lavergnat J., & Golé P. (1998). A stochastic raindrop time distribution model. *Journal of Applied Meteorology*, *37*(8), 805–818.

Mandeep J. S., Allnut J. E. (2007). Rain attenuation predictions at Ku-band in south east Asia Countries. *Progress in Electromagnetics, PIERS,* 76, 65-74.

Ng Y., Singh M., Singh J., Thiruchelvam V. (2017). Performance analysis of 60-min to 1-min integration time rain rate conversion models in Malaysia. *Journal of Atmospheric and Solar-Terrestrial Physics*, 167, 13–22.

Ojo J. S., Ajewole M.O., Sarkar S.K. (2008). Rain rate and rain attenuation prediction for satellite communication in Ku and Ka bands over Nigeria. *Progress in Electromagnetics,* Res. B, 5, 207-223.

Oktaviani, R., Marzuki. (2019). Estimation of rainfall rate cumulative distribution in Indonesia using global satellite mapping of precipitation data. *International Conference on Basic Sciences and Its Applications*, 2019, 259–265.

Panchal P., Joshi R. (2016). Performance analysis and simulation of rain attenuation models at 12-40 GHz band for an earth space path over Indian cities. 7th Int. Conf. on Commun., Comput. and Virtualiz., *ScienceDirect*, 79, 801-808.

Pérez-García, N., Pinto, A.D., Torres, J.M., Rivera, Y.E., Mello, L.A.R. S, Garcia, R., Ramírez, E.J., Guevara-Salgado, P. (2023). Preliminary rain rate statistics with one-minute integration time for radio propagation uses in Venezuela. *Electronics Letters,* 59(6), 1-3.

Rafiqul I., Alam M., Lwas A. K., Mohamad S. Y. (2018). Rain rate distributions for microwave link design based on long term measurement in Malaysia. *Indonesian Journal of Electrical Engineering and Computer Science*, 10(3), 1023–1029.

Shrestha S., Park J., Choi, D. (2016). Rain rate modeling of 1-min from various integration times in South Korea. *SpringerPlus*, 5:433, 1-34.

Shrestha S., Choi D. (2017a). Characterization of rain specific attenuation and frequency scaling method for satellite communication in South Korea. *Int. J. of Antenn. and Propag*., 1-16.

Shrestha S., Choi D. (2017b). Study of 1-min rain rate integration statistics in South Korea. *J. of Atm. and Solar-Terr. Phys*., 155, 1–11.

Shrestha S., Choi D. (2018). Diurnal and monthly variations of rain rate and rain attenuation on Ka-band satellite communication in South Korea. *Prog. In Electromagn. Res. B*, 80, 151-171.

Singh R., Acharya R. (2019). Development of a new global model for estimating one-minute rainfall rate. *IEEE Transactions on Geoscience and Remote Sensing*, 56(11), 6462–6468.

Stutzman W.L., Dishman W.K. (1984). Correction to a simple model for the estimation of rain-induced attenuation along earth-space paths at millimeter wavelengths. *Rad. Sci*., 19, 946.

Svjatogor L. (1985). Prostranstvennaia korelacia vypadenjija dozdjej vdol zemnoj poverchnostji (in Russian), Symposium expertov stran uchastnic programmy *INTERKOSMOS* (Interkosmos symposium, theme 5 of the established telecommunication working group, Dresden, GDR).

Tamosiunaite M., Tamosiuniene M., Gruodis A., Tamosiunas S., 2010. Prediction of electromagnetic wave attenuation due to water in the atmosphere. 1. Attenuation due to rain. *Innov. Infotech. for Sci, Business and Edu*., ISSN 2029-1035, 2(9), 3-10.

DOI:https//doi.org/10.22452/mjs.vol43no3.13
Malaysian Journal of Science 43(3): 119-127 (September 2024)